International Journal of Multidisciplinary and Current Research ISSN: 2321-3124
Review Article Available at: http://ijmcr.com

Analysis of Simply Supported Laminated Plate Using CLT and FSDT

Dharmender Jangra*

Department of Mechanical and Automation Engineering, Northern India Engineering College, New Delhi, India

Received 30 Sept 2022, Accepted 10 Oct 2022, Available online 17 Oct 2022, **Vol.10 (Sept/Oct 2022 issue)**

Abstract

Composite is the special kind of engineered materials. The mechanics of the composite are a little bit complicated. In the present work, the classical laminate theory (CLT) and first-order shear deformation theory (FSDT) is used for the finding the deformation/deflection in the simply supported composite plate loaded with the uniformly distributed load. The Navier solution applied to find the desired result.

Keywords: *Composite, Lamina, Laminate, Stacking Sequence*

1. Introduction

Composite materials are those that are made by combining two or more materials on a macroscopic scale in such a way that they have enhanced engineering qualities than the standard materials, such as metals. These materials are known as "composite materials." Stiffness, strength, resistance to corrosion, thermal characteristics, fatigue life, wear resistance [1-28], and effective decrease in weight are some of the attributes that may be enhanced. The vast majority of man-made composite materials are constructed using two different kinds of materials: a substance known as fibre for providing reinforcement and a material known as matrix material serving as the foundation or parent material. A typical sheet made of composite material is referred to as a lamina or ply. It is a vital component that makes up the whole. Numerous fibres are implanted in a matrix material to create a fiber-reinforced lamina [29-43]. This matrix material may be made of a metal, such as aluminium, or it can be made of a non-metal, such as thermoset or thermoplastic polymer. A laminate is a collection of lamina that have been layered in order to obtain the necessary stiffness and thickness. For example, lamina that are reinforced with unidirectional fibres may be stacked in such a way that the fibres in each lamina are orientated in the same or opposite directions. Both the laminates and the materials benefit from an improvement in their tribological characteristics as a result of the orientation [44-86]. Gears and other machine components often make use of the composite material. There have been a number of researches [87-159] conducted on the topic of gear failure as well as design and dependability. As a result, it is essential to do research on composites since they are a potential future material.

*Corresponding author's ORCID ID: 0000-0000-0000-0000
DOI: https://doi.org/10.14741/ijmcr/v.10.5.3

The orientation of the plies determines the two distinct kinds of laminates that may be created. [160]

A. Angle Ply

Angle-ply laminates have ply configurations of θ and - θ where 0° ≤ θ ≤90°, and at least one stack has an alignment other than 0° or 90°, as shown in Fig. 1.

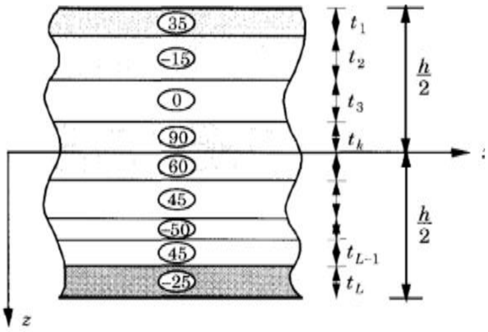

Fig.1 Angle ply laminates

B. Cross Ply

Cross-ply laminates are those which have ply orientations of 0° or 90° as shown in Fig. 2

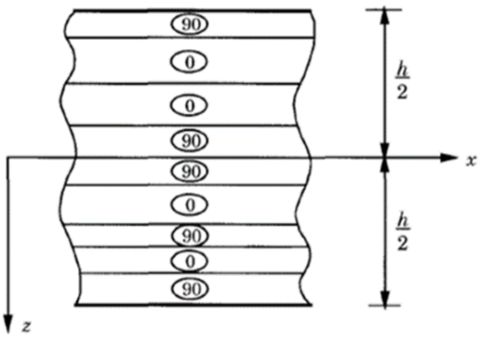

Fig. 2 Cross-ply laminate

2. Theories of analysis and their mathematical modelling

Calculating the deflection and stress in a composite plate may be done using a variety of different theories, such as the classical laminate plate theory, the first order shear deformation theory, the higher order shear deformation theory [8], and so on. In this part, we will construct the link between the classical laminate theory (CLT) and the first-order shear deformation theory (FSDT) utilising these two theories. and Navier solution is applied to find the desired result. [161]

A. Classical Laminate Plate Theory and Mathematical Modelling of CLT

Any orthotropic continuous fibre laminated composites may be explained by the Classical Lamination Theory (CLT), which is described in this article. The method that was used while developing CLT is quite comparable to the one that was applied when developing load-stress relationships in the fundamental courses on the strength of materials. It is presumed that there was an initial displacement field with loads that were applied. It is possible to characterise a state of stress by using the strain-displacement fields in conjunction with an appropriate constitutive connection. After ensuring that the criteria of static equilibrium are met, one may establish a load-strain relation and, as a consequence of this, one can define a state of stress for each lamina [162].

Fundamental Presuppositions of the Traditional Lamination Theory (CLT)

- The laminate has layers that are each quasi-homogeneous and orthotropic in nature.
- When compared to the lateral dimensions, the laminate is rather thin, and it bears load in its plane.
- State of stress is plane stress.
- Any and all displacements are negligible in comparison to the thickness of the laminate.
- There is no break in the displacements anywhere inside the laminate.
- After deformation, straight lines that are normal to the centre surface keep their straightness and maintain their normality to that surface.
- In-plane displacements vary linearly through the thickness,
- Transverse shear strains (γ_{xz} & γ_{yz}) are negligible.
- Transverse normal strain ε_z is negligible compared to the in-plane strains ε_x and ε_y.
- Strain-displacement and stress-strain relations are linear.

The centre of the plate, also known as z = 0, serves as the point of origin for the plate. Assume that u0, v0, and w0 are the displacements in the x, y, and z directions, respectively, at the midplane, and that u, v, and w are the displacements at any point in the x, y, and z directions, respectively. u, v, and w are the displacements at any point in the x, y, and z directions, respectively. The two displacements in the x–y plane at any point other than the midplane will rely on the axial position of the point as well as the slope of the laminate midplane with respect to the x and y directions [163].

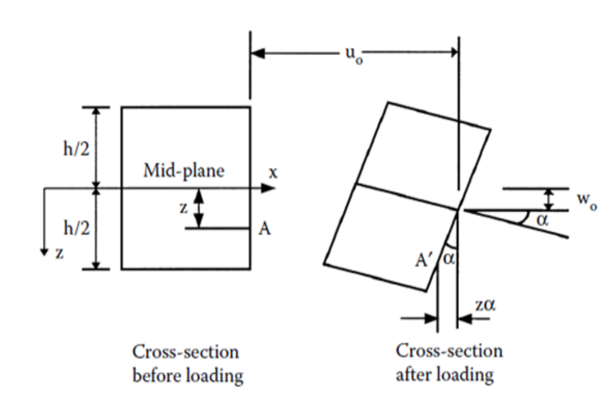

Fig. 3 Bending of the ply

Displacement in x and y-direction

$$u = u_0 - z\frac{\partial w_0}{\partial x} \quad (1)$$

$$v = v_0 - z\frac{\partial w_0}{\partial y} \quad (2)$$

Strain-displacement equation can be written in matrix form as in equation (3).

$$\begin{Bmatrix} \varepsilon_x \\ \varepsilon_y \\ \gamma_{xy} \end{Bmatrix} = \begin{Bmatrix} \frac{\partial u_0}{\partial x} \\ \frac{\partial v_0}{\partial y} \\ \frac{\partial u_0}{\partial x} + \frac{\partial v_0}{\partial y} \end{Bmatrix} + z \begin{Bmatrix} -\frac{\partial^2 w_0}{\partial x^2} \\ -\frac{\partial^2 w_0}{\partial y^2} \\ -\frac{\partial^2 w_0}{\partial x \partial y} \end{Bmatrix} \quad (3)$$

$$\begin{Bmatrix} \varepsilon_x \\ \varepsilon_y \\ \gamma_{xy} \end{Bmatrix} = \begin{Bmatrix} \varepsilon_x^o \\ \varepsilon_y^o \\ \gamma_{xy}^o \end{Bmatrix} + z \begin{Bmatrix} k_x \\ k_y \\ k_{xy} \end{Bmatrix} \quad (4)$$

The governing equations consist of the behavior of the boundary conditions as well as the behavior of the plate internally. The governing differential equations will be derived by summing the forces and moments on the plate.

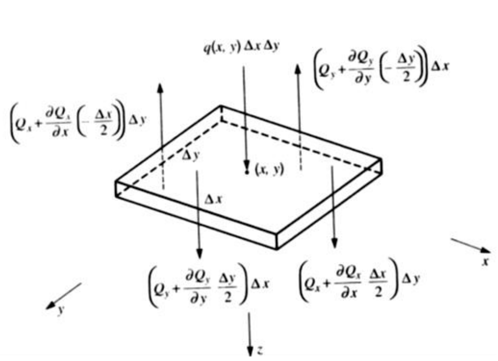

Fig. 4 Forces in z-direction

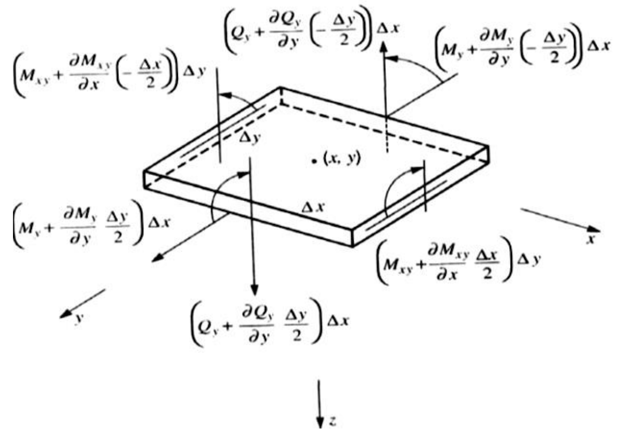

Fig. 5 Moment on the plate

The governing equation can be obtained by the summing up the forces and moment in x and y-direction

$$\frac{\partial N_x}{\partial x}+\frac{\partial N_{xy}}{\partial y}=0 \qquad (5)$$

$$\frac{\partial N_{xy}}{\partial x}+\frac{\partial N_y}{\partial x}=0 \qquad (6)$$

$$\frac{\partial^2 M_x}{\partial x^2}+\frac{\partial^2 M_{xy}}{\partial x \partial y}+\frac{\partial^2 M_x}{\partial y^2}+q=0 \qquad (7)$$

The equilibrium equation in terms of displacement is as

$$A_{11}\frac{\partial^2 u^o}{\partial x^2}+2A_{16}\frac{\partial^2 u^o}{\partial x \partial y}+A_{66}\frac{\partial^2 u^o}{\partial y^2}+(A_{12}+A_{66})\frac{\partial^2 v^o}{\partial x \partial y} +A_{26}\frac{\partial^2 u^o}{\partial y^2}-B_{11}\frac{\partial^3 w^o}{\partial x^3}-3B_{16}\frac{\partial^3 w^o}{\partial x^2 \partial y}- (B_{12}+B_{66})\frac{\partial^3 w^o}{\partial y^2 \partial x}-B_{26}\frac{\partial^3 w^o}{\partial y^3}=0 \qquad (8)$$

$$A_{16}\frac{\partial^2 u^o}{\partial x^2}+(A_{12}+A_{66})\frac{\partial^2 u^o}{\partial x \partial y}+A_{26}\frac{\partial^2 u^o}{\partial y^2}+A_{66}\frac{\partial^2 v^o}{\partial x^2}+ 2A_{26}\frac{\partial^2 v^o}{\partial x \partial y}+A_{22}\frac{\partial^2 u^o}{\partial y^2}-B6\frac{\partial^3 w^o}{\partial x^3}-(B_{12}+2B_{66})\frac{\partial^3 w^o}{\partial x^2 \partial y} -3B_{26}\frac{\partial^3 w^o}{\partial y^2 \partial x}-B_{26}\frac{\partial^3 w^o}{\partial y^3}=0 \qquad (9)$$

$$D_{11}\frac{\partial^4 w^0}{\partial x^4}+4D_{16}\frac{\partial^4 w^0}{\partial x^3 \partial y}+2(D_{12}+2D_{66})\frac{\partial^4 w^0}{\partial x^2 \partial y^2} +4D_{26}\frac{\partial^4 w^0}{\partial x \partial y^3}+D_{22}\frac{\partial^4 w^0}{\partial y^4}-B_{11}\frac{\partial^3 u^o}{\partial x^3}-3B_{16}\frac{\partial^3 u^o}{\partial x^2 \partial y} -(B_{12}+2B_{66})\frac{\partial^3 u^o}{\partial y^2 \partial x}-B_{26}\frac{\partial^3 u^o}{\partial y^3}-B_{16}\frac{\partial^3 v^o}{\partial x^3} -(B_{12}+2B_{66})\frac{\partial^3 v^o}{\partial x^2 \partial y}-3B_{26}\frac{\partial^3 v^o}{\partial y^2 \partial x}-B_{22}\frac{\partial^3 v^o}{\partial y^3}=0 \qquad (10)$$

Navier solution for CLT

Load and the displacement are considered in the form of furrier transform

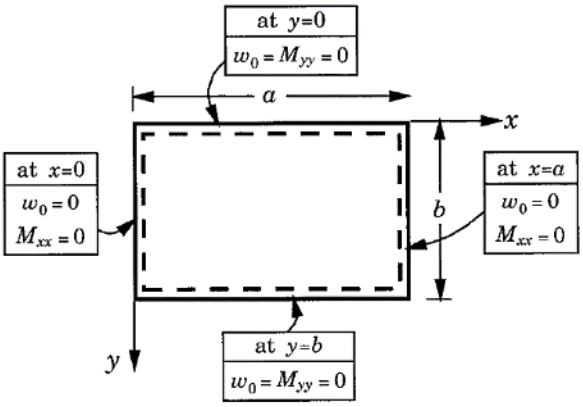

Fig. 6 Boundary condition for CLT

Boundary condition

$$w_0(x,0)=0 \qquad w_0(x,b)=0$$

$$w_0(0,y)=0 \qquad w_0(a,y)=0$$

$$M_{yy}(x,0)=0 \qquad M_{xx}(0,y)=0$$

$$M_{yy}(x,b)=0 \qquad M_{xx}(a,y)=0 \qquad (11)$$

$$w_0(x,y)=\sum_{n=1}^{\infty}\sum_{m=1}^{\infty} W_{mn}\sin\frac{m\pi}{a}x\sin\frac{n\pi}{b}y \qquad (12)$$

$$q_0(x,y)=\sum_{n=1}^{\infty}\sum_{m=1}^{\infty} Q_{mn}\sin\frac{m\pi}{a}x\sin\frac{n\pi}{b}y \qquad (13)$$

Where $q_0(x,y)$ represent the load value.

$$Q_{mn}=\frac{4}{ab}\int_0^b\int_0^a q(x,y)\sin\frac{m\pi}{a}x\sin\frac{n\pi}{b}y\,dx\,dy \qquad (14)$$

The forces and moments can be expressed as

$$\begin{Bmatrix} N_x \\ N_y \\ N_{xy} \\ M_x \\ M_y \\ M_{xy} \end{Bmatrix} = \begin{bmatrix} A_{11} & A_{12} & A_{13} & B_{11} & B_{12} & B_{13} \\ A_{22} & A_{21} & A_{23} & B_{22} & B_{21} & B_{23} \\ A_{13} & A_{32} & A_{33} & B_{13} & B_{32} & B_{33} \\ B_{11} & B_{12} & B_{13} & D_{11} & D_{12} & D_{13} \\ B_{22} & B_{21} & B_{23} & D_{22} & D_{21} & D_{23} \\ B_{13} & B_{32} & B_{33} & B_{13} & B_{32} & B_{33} \end{bmatrix} \begin{Bmatrix} \varepsilon_x^o \\ \varepsilon_y^o \\ \gamma_{xy}^o \\ k_x \\ k_y \\ k_{xy} \end{Bmatrix} \qquad (15)$$

B. First-Order Shear Deformation Theory and Mathematical Modelling of FSDT

During the mathematical modeling of the CLT we take many assumptions, now for FSDT some of the assumptions are relaxed to get more practical results.[163]

The only assumption relaxed for FSDT is that the perpendicular to the mid-surface plane is not remained normal after the deformation [164-167].

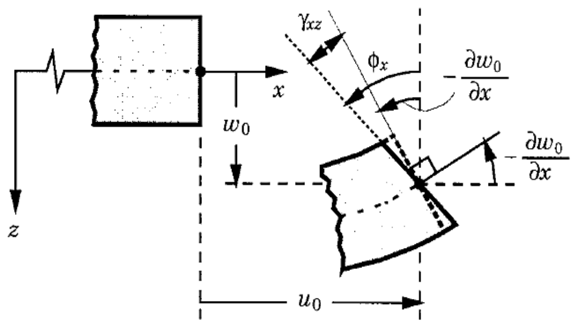

Fig. 7 Bending of ply in FSDT the normal is not remain normal to mid surface after deformation

Displacements are given by

$$u(x,y,z,t) = u_o(x,y,z,t) + z\varphi_x(x,y,t) \quad (16)$$
$$v(x,y,z,t) = v_o(x,y,z,t) + z\varphi_y(x,y,t) \quad (17)$$
$$z(x,y,z,t) = z_o(x,y,z,t) \quad (18)$$

$$\varphi_x = \frac{\partial u}{\partial z} \qquad \varphi_y = \frac{\partial v}{\partial z} \quad (19)$$

$$\begin{Bmatrix}\varepsilon_{xx}\\ \varepsilon_{yy}\\ \gamma_{yz}\\ \gamma_{xz}\\ \gamma_{xy}\end{Bmatrix} = \begin{Bmatrix}\frac{\partial u_0}{\partial x}+\frac{1}{2}\left(\frac{\partial w_0}{\partial x}\right)^2\\ \frac{\partial v_0}{\partial y}+\frac{1}{2}\left(\frac{\partial w_0}{\partial y}\right)^2\\ \frac{\partial w_0}{\partial y}+\varphi_y\\ \frac{\partial w_0}{\partial x}+\varphi_x\\ \frac{\partial u_0}{\partial y}+\frac{\partial v_0}{\partial x}+\frac{\partial w_0}{\partial y}\frac{\partial w_0}{\partial x}\end{Bmatrix} + z\begin{Bmatrix}\frac{\partial \varphi_x}{\partial x}\\ \frac{\partial \varphi_y}{\partial y}\\ 0\\ 0\\ \frac{\partial \varphi_x}{\partial y}+\frac{\partial \varphi_y}{\partial x}\end{Bmatrix}$$

(20)

The equilibrium equation in terms of displacement is as

$$\frac{\partial}{\partial x}[A_{11}\frac{\partial u_0}{\partial x} + A_{12}\frac{\partial v_0}{\partial y} + A_{16}\left(\frac{\partial u_0}{\partial y}+\frac{\partial v_0}{\partial x}\right) + B_{11}\frac{\partial \varphi_x}{\partial x}$$
$$+B_{12}\frac{\partial \varphi_y}{\partial y} + B_{16}\left(\frac{\partial \varphi_x}{\partial y}+\frac{\partial \varphi_y}{\partial x}\right)] + \frac{\partial}{\partial y}[A_{16}\frac{\partial u_0}{\partial x}$$
$$+A_{26}\frac{\partial v_0}{\partial y} + A_{66}\left(\frac{\partial u_0}{\partial y}+\frac{\partial v_0}{\partial x}\right) + B_{16}\frac{\partial \varphi_x}{\partial x}$$
$$+B_{26}\frac{\partial \varphi_y}{\partial y} + B_{66}\left(\frac{\partial \varphi_x}{\partial y}+\frac{\partial \varphi_y}{\partial x}\right)]$$
$$-\left(\frac{\partial N_{xx}^T}{\partial x}+\frac{\partial N_{xy}^T}{\partial y}\right) = I_o\frac{\partial^2 u_0}{\partial t^2} + I_1\frac{\partial^2 \varphi_x}{\partial t^2}$$

(21)

$$\frac{\partial}{\partial x}[A_{16}\frac{\partial u_0}{\partial x} + A_{26}\frac{\partial v_0}{\partial y} + A_{66}\left(\frac{\partial u_0}{\partial y}+\frac{\partial v_0}{\partial x}\right) + B_{16}\frac{\partial \varphi_x}{\partial x}$$
$$+B_{26}\frac{\partial \varphi_y}{\partial y} + B_{66}\left(\frac{\partial \varphi_x}{\partial y}+\frac{\partial \varphi_y}{\partial x}\right)] + \frac{\partial}{\partial y}[A_{12}\frac{\partial u_0}{\partial x}$$
$$+A_{22}\frac{\partial v_0}{\partial y} + A_{26}\left(\frac{\partial u_0}{\partial y}+\frac{\partial v_0}{\partial x}\right) + B_{12}\frac{\partial \varphi_x}{\partial x}$$
$$+B_{22}\frac{\partial \varphi_y}{\partial y} + B_{26}\left(\frac{\partial \varphi_x}{\partial y}+\frac{\partial \varphi_y}{\partial x}\right)]$$
$$-\left(\frac{\partial N_{xy}^T}{\partial x}+\frac{\partial N_{yy}^T}{\partial y}\right) = I_o\frac{\partial^2 v_0}{\partial t^2} + I_1\frac{\partial^2 \varphi_y}{\partial t^2} \quad (22)$$

$$\frac{\partial}{\partial x}[KA_{45}(\frac{\partial w_0}{\partial y}+\varphi_y) + KA_{55}(\frac{\partial w_0}{\partial x}+\varphi_x)]$$
$$+\frac{\partial}{\partial y}[KA_{44}(\frac{\partial w_0}{\partial y}+\varphi_y) + KA_{45}(\frac{\partial w_0}{\partial x}+\varphi_x)]$$
$$+\widehat{N}_{xx}\frac{\partial^2 w_0}{\partial x^2} + \widehat{N}_{yy}\frac{\partial^2 w_0}{\partial y^2} + 2\widehat{N}_{xy}\frac{\partial^2 w_0}{\partial x\partial y} + q$$
$$= I_o\frac{\partial^2 w_0}{\partial t^2} \quad (23)$$

$$\frac{\partial}{\partial x}[B_{11}\frac{\partial u_0}{\partial x} + B_{12}\frac{\partial v_0}{\partial y} + B_{16}(\frac{\partial u_0}{\partial y}+\frac{\partial v_0}{\partial x})$$
$$+D_{11}\frac{\partial \varphi_x}{\partial x} + D_{12}\frac{\partial \varphi_y}{\partial y} + D_{16}(\frac{\partial \varphi_x}{\partial y}+\frac{\partial \varphi_y}{\partial x})$$
$$+\frac{\partial}{\partial y}[B_{16}\frac{\partial u_0}{\partial x} + B_{26}\frac{\partial v_0}{\partial y} + B_{66}(\frac{\partial u_0}{\partial y}+\frac{\partial v_0}{\partial x})$$
$$+D_{16}\frac{\partial \varphi_x}{\partial x} + D_{26}\frac{\partial \varphi_y}{\partial y} + D_{66}(\frac{\partial \varphi_x}{\partial y}+\frac{\partial \varphi_y}{\partial x})$$
$$-[KA_{45}(\frac{\partial w_0}{\partial y}+\varphi_y) + KA_{55}(\frac{\partial w_0}{\partial x}+\varphi_x)]$$
$$-\left(\frac{\partial M_{xx}^T}{\partial x}+\frac{\partial M_{xy}^T}{\partial y}\right) = I_2\frac{\partial^2 \varphi_x}{\partial t^2} + I_1\frac{\partial^2 u_0}{\partial t^2} \quad (24)$$

$$\frac{\partial}{\partial x}[B_{16}\frac{\partial u_0}{\partial x} + B_{26}\frac{\partial v_0}{\partial y} + B_{66}(\frac{\partial u_0}{\partial y}+\frac{\partial v_0}{\partial x})$$
$$+D_{16}\frac{\partial \varphi_x}{\partial x} + D_{26}\frac{\partial \varphi_y}{\partial y} + D_{66}(\frac{\partial \varphi_x}{\partial y}+\frac{\partial \varphi_y}{\partial x})$$
$$+\frac{\partial}{\partial y}[B_{12}\frac{\partial u_0}{\partial x} + B_{22}\frac{\partial v_0}{\partial y} + B_{26}(\frac{\partial u_0}{\partial y}+\frac{\partial v_0}{\partial x})$$
$$+D_{12}\frac{\partial \varphi_x}{\partial x} + D_{22}\frac{\partial \varphi_y}{\partial y} + D_{26}(\frac{\partial \varphi_x}{\partial y}+\frac{\partial \varphi_y}{\partial x})$$
$$-[KA_{44}(\frac{\partial w_0}{\partial y}+\varphi_y) + KA_{45}(\frac{\partial w_0}{\partial x}+\varphi_x)]$$
$$-\left(\frac{\partial M_{xy}^T}{\partial x}+\frac{\partial M_{yy}^T}{\partial y}\right) = I_2\frac{\partial^2 \varphi_y}{\partial t^2} + I_1\frac{\partial^2 v_0}{\partial t^2} \quad (25)$$

Navier solution for FSDT

Load and the displacement are considered in the form of furrier transform

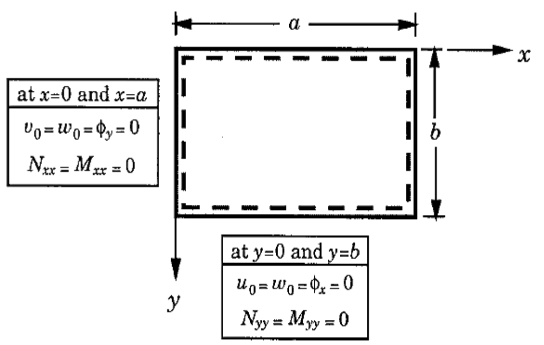

Fig. 8 Boundary condition for FSDT

Boundary condition

$$w_0(x,0,t) = 0 \quad w_0(x,b,t) = 0$$
$$w_0(0,y,t) = 0 \quad w_0(a,y,t) = 0$$
$$u_0(x,0,t) = 0 \quad u_0(x,b,t) = 0$$
$$v_0(0,y,t) = 0 \quad v_0(a,y,t) = 0$$

$$M_{yy}(x,0,t) = 0 \;\; M_{yy}(x,b,t) = 0$$
$$M_{xx}(0,y,t) = 0 \;\; M_{xx}(a,y,t) = 0$$
$$N_{yy}(x,0,t) = 0 \;\; N_{yy}(x,b,t) = 0$$
$$N_{xx}(0,y,t) = 0 \;\; N_{xx}(a,y,t) = 0$$
$$\varphi_x(x,0,t) = 0 \;\; \varphi_x(x,b,t) = 0$$
$$\varphi_y(o,y,t) = 0 \;\; \varphi_y(a,y,t) = 0 \qquad (26)$$

$$w_0(x,y,t) = \sum_{n=1}^{\infty}\sum_{m=1}^{\infty} W_{mn}(t)\sin\frac{m\pi}{a}x\sin\frac{n\pi}{b}y \qquad (27)$$

$$u_0(x,y,t) = \sum_{n=1}^{\infty}\sum_{m=1}^{\infty} U_{mn}(t)\cos\frac{m\pi}{a}x\sin\frac{n\pi}{b}y \qquad (28)$$

$$v_0(x,y,t) = \sum_{n=1}^{\infty}\sum_{m=1}^{\infty} V_{mn}\sin\frac{m\pi}{a}x\cos\frac{n\pi}{b}y \qquad (29)$$

$$\varphi_x(x,y,t) = \sum_{n=1}^{\infty}\sum_{m=1}^{\infty} X_{mn}\cos\frac{m\pi}{a}x\sin\frac{n\pi}{b}y \qquad (30)$$

$$\varphi_y(x,y,t) = \sum_{n=1}^{\infty}\sum_{m=1}^{\infty} Y_{mn}\cos\frac{m\pi}{a}x\sin\frac{n\pi}{b}y \qquad (31)$$

$$q(x,y,t) = \sum_{n=1}^{\infty}\sum_{m=1}^{\infty} Q_{mn}(t)\sin\frac{m\pi}{a}x\sin\frac{n\pi}{b}y \qquad (32)$$

The deflection can be expressed as

$$\begin{bmatrix} \hat{S}_{11} & \hat{S}_{12} & 0 & \hat{S}_{14} & \hat{S}_{15} \\ \hat{S}_{12} & \hat{S}_{22} & 0 & \hat{S}_{24} & \hat{S}_{25} \\ 0 & 0 & \hat{S}_{33} & \hat{S}_{34} & \hat{S}_{35} \\ \hat{S}_{14} & \hat{S}_{24} & \hat{S}_{34} & \hat{S}_{44} & \hat{S}_{45} \\ \hat{S}_{15} & \hat{S}_{25} & \hat{S}_{35} & \hat{S}_{45} & \hat{S}_{55} \end{bmatrix} \begin{Bmatrix} U_{mn} \\ V_{mn} \\ W_{mn} \\ X_{mn} \\ Y_{mn} \end{Bmatrix} = \begin{Bmatrix} 0 \\ 0 \\ Q_{mn} \\ 0 \\ 0 \end{Bmatrix} \qquad (33)$$

Where stiffness matrix is the function of the A, B and D matrix, Q_{mn} is load coefficient.[165]

3. Result and discussion

The analysis of simply supported composite plate is done with the Matlab programming. The mathematical modeling is done for the plate and Navier solution is found out. The non-dimensional parameters are plotted against each other like the ratio of plate width to thickness plotted against the deflection, modulus ratio also plotted against deflection, the effect of the ply angle and the number of layers also plotted.

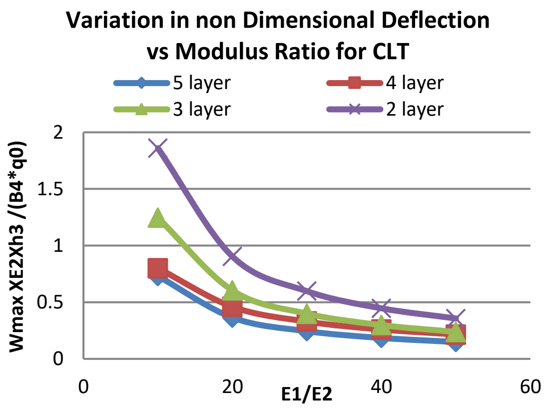

Fig.9 Variation of non-dimensional deflection with respect to modulus ratio for CLT

In above Fig. 9 as the number of layers are increasing the non-dimensional deflection is decreasing, Also, as the modulus ratio is increasing the non-dimensional deflection is decreasing. If the modulus ratio is less the 20 the non-dimensional deflection is high and considerable variation with respect to the number of layers.

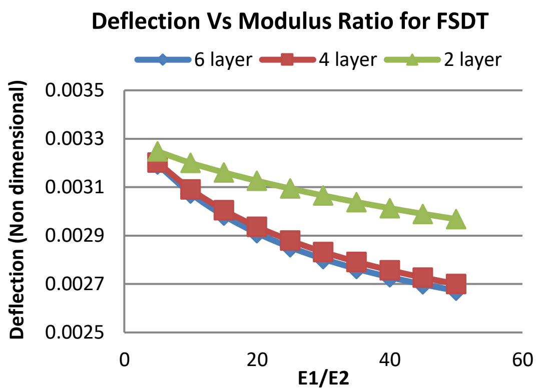

Fig. 10 Non- dimensional deflection variation with respect to modulus ratio for FSDT

From Fig.10 as the number of layers are increasing the deflection is decreasing and also as the modulus ratio is increasing the deflection is also decreasing.

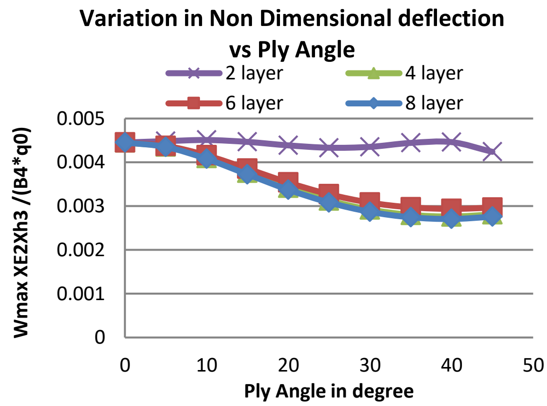

Fig. 11 Non- dimensional deflection variation with respect to ply angle for CLT

From Fig.11 the non-dimensional deflection is decreasing as the ply angle is increasing. As the number of layers is increasing the deflection is affected less or there is less amount of deflection.

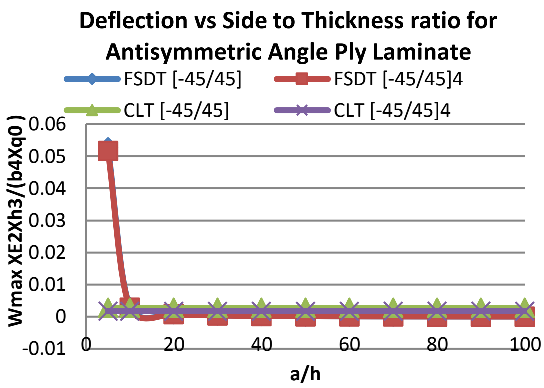

Fig. 12 Non- dimensional deflection variation with respect to width to thickness ratio for antisymmetric angle-ply laminate for CLT and FSDT

From the Fig.12 the variation in the deflection is less when the ratio(a/h) is more the 20. If the ratio is less than 20 the variation of deflection For FSDT is higher than the CLT. When two stacking sequence and the more are taken the variation shown by the CLT is remains constant means not such a considerable change is there but as for the FSDT the change is considerable if the side to thickness ratio (a/h) is below 20.

Conclusions

The above analysis shows that the first order shear deformation theory gives better results than classical laminate theory. The difference is very high for the side to thickness ratio if less than 20. The deflection should increase as the modulus ratio increase. If the number of layers increasing the deflection decreasing. The program made for this is generalized one the output trend will be always same for the inputs.

References

[1]. Hirani, H., & Suh, N. P. (2005). Journal bearing design using multiobjective genetic algorithm and axiomatic design approaches. *Tribology International*, *38*(5), 481-491.

[2]. Hirani, H., & Verma, M. (2009). Tribological study of elastomeric bearings for marine propeller shaft system. *Tribology international*, *42*(2), 378-390.

[3]. Samanta, P., & Hirani, H. (2008). Magnetic bearing configurations: Theoretical and experimental studies. *IEEE transactions on magnetics*, *44*(2), 292-300.

[4]. Sukhwani, V. K., & Hirani, H. (2008). Design, development, and performance evaluation of high-speed magnetorheological brakes. *Proceedings of the Institution of Mechanical Engineers, Part L: Journal of Materials: Design and Applications*, *222*(1), 73-82.

[5]. Sarkar, C., & Hirani, H. (2013). Theoretical and experimental studies on a magnetorheological brake operating under compression plus shear mode. *Smart Materials and Structures*, *22*(11), 115032.

[6]. Hirani, H., Athre, K., and Biswas, S. (October 1, 1999). "Dynamically Loaded Finite Length Journal Bearings: Analytical Method of Solution." ASME. *J. Tribol*. October 1999; 121(4): 844–852. https://doi.org/10.1115/1.2834144

[7]. Hirani, H., Rao, T. V. V. L. N., Athre, K., & Biswas, S. (1997). Rapid performance evaluation of journal bearings. *Tribology international*, *30*(11), 825-834.

[8]. Sukhwani, V. K., & Hirani, H. (2008). A comparative study of magnetorheological-fluid-brake and magnetorheological-grease-brake. *Tribology Online*, *3*(1), 31-35.

[9]. Muzakkir, S. M., Lijesh, K. P., & Hirani, H. (2014). Tribological failure analysis of a heavily-loaded slow speed hybrid journal bearing. *Engineering Failure Analysis*, *40*, 97-113.

[10]. Sarkar, C., & Hirani, H. (2013, February). Design of a squeeze film magnetorheological brake considering compression enhanced shear yield stress of magnetorheological fluid. In *Journal of Physics: Conference Series* (Vol. 412, No. 1, p. 012045). IOP Publishing.

[11]. KP, L., & Hirani, H. (2014). Stiffness and damping coefficients for rubber mounted hybrid bearing. *Lubrication Science*, *26*(5), 301-314.

[12]. Rao, T. V. V. L. N., Biswas, S., Hirani, H., & Athre, K. (2000). An analytical approach to evaluate dynamic coefficients and nonlinear transient analysis of a hydrodynamic journal bearing. *Tribology transactions*, *43*(1), 109-115.

[13]. Sarkar, C., & Hirani, H. (2013). Synthesis and characterization of antifriction magnetorheological fluids for brake. *Defence science journal*, *63*(4), 408.

[14]. Hirani, H., & Samanta, P. (2007). Hybrid (hydrodynamic+ permanent magnetic) journal bearings. *Proceedings of the Institution of Mechanical Engineers, Part J: Journal of Engineering Tribology*, *221*(8), 881-891.

[15]. Hirani, H. (2004). Multiobjective optimization of a journal bearing using the Pareto optimality concept. *Proceedings of the Institution of Mechanical Engineers, Part J: Journal of Engineering Tribology*, *218*(4), 323-336.

[16]. Muzakkir, S. M., Hirani, H., Thakre, G. D., & Tyagi, M. R. (2011). Tribological failure analysis of journal bearings used in sugar mills. *Engineering Failure Analysis*, *18*(8), 2093-2103.

[17]. Hirani, H. (2016). *Fundamentals of engineering tribology with applications*. Cambridge University Press.

[18]. Sarkar, C., & Hirani, H. (2015). Effect of particle size on shear stress of magnetorheological fluids. *Smart Science*, *3*(2), 65-73.

[19]. Sarkar, C., & Hirani, H. (2015). Development of a magnetorheological brake with a slotted disc. *Proceedings of the Institution of Mechanical Engineers, Part D: Journal of Automobile Engineering*, *229*(14), 1907-1924.

[20]. Lijesh, K. P., & Hirani, H. (2015). Optimization of eight pole radial active magnetic bearing. *Journal of Tribology*, *137*(2), 024502.

[21]. Muzakkir, S. M., Hirani, H., & Thakre, G. D. (2013). Lubricant for heavily loaded slow-speed journal bearing. *Tribology transactions*, *56*(6), 1060-1068.

[22]. Hirani, H., & Goilkar, S. S. (2009). Formation of transfer layer and its effect on friction and wear of carbon–graphite face seal under dry, water and steam environments. *Wear*, *266*(11-12), 1141-1154.

[23]. Hirani, H., Athre, K., & Biswas, S. (1998). Rapid and globally convergent method for dynamically loaded journal bearing design. *Proceedings of the Institution of Mechanical Engineers, Part J: Journal of Engineering Tribology*, *212*(3), 207-214.

[24]. Muzakkir, S. M., Lijesh, K. P., Hirani, H., & Thakre, G. D. (2015). Effect of cylindricity on the tribological performance of heavily loaded slow-speed journal bearing. *Proceedings of the Institution of Mechanical Engineers, Part J: Journal of Engineering Tribology*, *229*(2), 178-195.

[25]. Lijesh, K. P., & Hirani, H. (2015). Development of analytical equations for design and optimization of axially polarized radial passive magnetic bearing. *Journal of Tribology*, *137*(1), 011103.

[26]. Lijesh, K. P., Muzakkir, S. M., & Hirani, H. (2015). Experimental tribological performance evaluation of nano lubricant using multi-walled carbon nano-tubes (MWCNT). *Int J Appl Eng Res*, *10*(6), 14543-14550.

[27]. Hirani, H. (2005). Multiobjective optimization of journal bearing using mass conserving and genetic algorithms. *Proceedings of the Institution of Mechanical*

Engineers, Part J: Journal of Engineering Tribology, *219*(3), 235-248.
[28]. Hirani, H., Athre, K., & Biswas, S. (2000). Comprehensive design methodology for an engine journal bearing. *Proceedings of the Institution of Mechanical Engineers, Part J: Journal of Engineering Tribology*, *214*(4), 401-412.
[29]. "Polymer Composites - 2021 - Antil - An Improvement in Drilling of SiCp Glass Fiber-reinforced Polymer Matrix Composites.Pdf."
[30]. Antil, P., Singh, S., and Singh, P. J., 2018, "Taguchi's Methodology Based Electrochemical Discharge Machining of Polymer Matrix Composites," Procedia Manuf., **26**, pp. 469–473.
[31]. Antil, P., Singh, S., and Manna, A., 2020, "Experimental Investigation During Electrochemical Discharge Machining (ECDM) of Hybrid Polymer Matrix Composites," Iran. J. Sci. Technol. - Trans. Mech. Eng., **44**(3), pp. 813–824.
[32]. Antil, P., Kumar Antil, S., Prakash, C., Królczyk, G., and Pruncu, C., 2020, "Multi-Objective Optimization of Drilling Parameters for Orthopaedic Implants," Meas. Control (United Kingdom), **53**(9–10), pp. 1902–1910.
[33]. Antil, P., Singh, S., Kumar, S., Manna, A., and Katal, N., 2019, "Taguchi and Multi-Objective Genetic Algorithm-Based Optimization during Ecdm of Sicp /Glass Fibers Reinforced Pmcs," Indian J. Eng. Mater. Sci., **26**(3–4), pp. 211–219.
[34]. Antil, P., Singh, S., and Manna, A., 2018, "SiCp/Glass Fibers Reinforced Epoxy Composites: Wear and Erosion Behavior," Indian J. Eng. Mater. Sci., **25**(2), pp. 122–130.
[35]. Antil, P., Singh, S., and Manna, A., 2019, "Analysis on Effect of Electroless Coated SiCp on Mechanical Properties of Polymer Matrix Composites," Part. Sci. Technol., **37**(7), pp. 787–794.
[36]. Antil, P., Singh, S., and Manna, A., 2018, "Genetic Algorithm Based Optimization of ECDM Process for Polymer Matrix Composite," Mater. Sci. Forum, **928 MSF**, pp. 144–149.
[37]. Antil, P., 2020, "Modelling and Multi-Objective Optimization during ECDM of Silicon Carbide Reinforced Epoxy Composites," Silicon, **12**(2), pp. 275–288.
[38]. Kharb, S. S., Antil, P., Singh, S., Antil, S. K., Sihag, P., and Kumar, A., 2021, "Machine Learning-Based Erosion Behavior of Silicon Carbide Reinforced Polymer Composites," Silicon, **13**(4), pp. 1113–1119.
[39]. Antil, P., 2019, "Experimental Analysis on Wear Behavior of PMCs Reinforced with Electroless Coated Silicon Carbide Particulates," Silicon, **11**(4), pp. 1791–1800.
[40]. Antil, P., Singh, S., and Manna, A., 2018, "Glass Fibers/SiCp Reinforced Epoxy Composites: Effect of Environmental Conditions," J. Compos. Mater., **52**(9), pp. 1253–1264.
[41]. Antil, P., Singh, S., Singh, S., Prakash, C., and Pruncu, C. I., 2019, "Metaheuristic Approach in Machinability Evaluation of Silicon Carbide Particle/Glass Fiber–Reinforced Polymer Matrix Composites during Electrochemical Discharge Machining Process," Meas. Control (United Kingdom), **52**(7–8), pp. 1167–1176.
[42]. Antil, S. K., Antil, P., Singh, S., Kumar, A., and Pruncu, C. I., 2020, "Artificial Neural Network and Response Surface Methodology Based Analysis on Solid Particle Erosion Behavior of Polymer Matrix Composites," Materials (Basel)., **13**(6).
[43]. Antil, P., Singh, S., Kumar, S., Manna, A., and Pruncu, C. I., 2019, "Erosion Analysis of Fiber Reinforced Epoxy Composites," Mater. Res. Express, **6**(10), p. 106520.
[44]. Desai, C., Hirani, H., & Chawla, A. (2015). Life estimation of hip joint prosthesis. *Journal of the Institution of Engineers (India): Series C*, *96*(3), 261-267.
[45]. Hirani, H., & Goilkar, S. S. (2011). Rotordynamic Analysis of Carbon Graphite Seals of a Steam Rotary Joint. In *IUTAM Symposium on Emerging Trends in Rotor Dynamics* (pp. 253-262). Springer, Dordrecht.
[46]. Hirani, H. (2009). Online Wear Monitoring of Spur Gear. *Indian Journal of Tribology*, *4*(2), 38-43.
[47]. Kumar, P., Hirani, H., & Agrawal, A. K. (2019). Modeling and simulation of mild wear of spur gear considering radial misalignment. *Iranian Journal of Science and Technology, Transactions of Mechanical Engineering*, *43*(1), 107-116.
[48]. Sarkar, C., & Hirani, H. (2017). Experimental studies on magnetorheological brake containing plane, holed and slotted discs. *Industrial Lubrication and Tribology*, *69*(2), 116-122.
[49]. Lijesh, K. P., & Hirani, H. (2017). Design and development of permanent magneto-hydrodynamic hybrid journal bearing. *Journal of Tribology*, *139*(4), 044501.
[50]. Hirani, H. (2012). Online Condition Monitoring of high speed gears using vibration and Oil Analysis. *Thermal Fluid and Manufacturing Science*.
[51]. Hirani, H., Athre, K., & Biswas, S. (2000). Transient trajectory of journal in hydrodynamic bearing. *Applied Mechanics and Engineering*, *5*(2), 405-418.
[52]. Sarkar, C., & Hirani, H. (2015). Synthesis and characterization of nano-particles based magnetorheological fluids for brake. *Tribology Online*, *10*(4), 282-294.
[53]. Hirani, H., & TVVLN, R. (2003). Optimization of journal bearing groove geometry using genetic algorithm. In *National Conference on Machines and Mechanism (NaCoMM)*.
[54]. Samanta, P., & Hirani, H. (2008, January). An overview of passive magnetic bearings. In *International Joint Tribology Conference* (Vol. 43369, pp. 465-467).
[55]. Samanta, P., Hirani, H., Mitra, A., Fernandes, B. G., & Kulkarni, A. M. (2005, December). Test setup for magnetohydrodynamic journal bearing. In *12th Nat. Conf. Machines and Mechanisms* (pp. 16-17).
[56]. Lijesh, K. P., Muzakkir, S. M., Hirani, H., & Thakre, G. D. (2016). Control on wear of journal bearing operating in mixed lubrication regime using grooving arrangements. *Industrial Lubrication and Tribology*.
[57]. Sukhwani, V. K., Hirani, H., & Singh, T. (2007, June). Synthesis and Performance Evaluation of Magnetorheological (MR) Grease. In *74th NLGI Annual Meeting, Scottsdale, Arizona, USA*.
[58]. Hirani, H., & Dani, S. (2005, January). Variable Valve Actuation Mechanism Using Magnetorheological Fluid. In *World Tribology Congress* (Vol. 42029, pp. 569-570).
[59]. Talluri, S. K., & Hirani, H. (2003). Parameter Optimization Of Journal Bearing Using Genetic Algorithm. *Indian Journal of Tribology*, *2*(1-2), 7-21.
[60]. Kumar, P., & Hirani, H. (2021). Misalignment effect on gearbox failure: An experimental study. *Measurement*, *169*, 108492.
[61]. Hirani, H., & Samanta, P. (2005, January). Performance Evaluation of Magnetohydrodynamic Bearing. In *World Tribology Congress* (Vol. 42029, pp. 97-98).
[62]. Samanta, P., & Hirani, H. (2022). On the evolution of passive magnetic bearings. *Journal of Tribology*, *144*(4).

[63]. Jangra D., Darpe, A. K., & Hirani, H. (2020, July). Classification of stages of wear in spur gears based on wear debris morphology. In *PHM Society European Conference* (Vol. 5, No. 1, pp. 9-9).
[64]. Hirani, H., Athre, K., & Biswas, S. (1999). Journal bearing design using TKSolver. *Applied Mechanics and Engineering*, *4*(spec.), 39-44.
[65]. Nag, S., Mondal, A., Hirani, H., Bhowmik, A. D., Chattopadhyay, A., & Banerjee, P. (2022). A dual-responsive bio-amicable fluorophore for trace level recognition of Zn2+ and Cd2+: Prefatory diagnosis of neoplastic disease from urine and ALS from saliva. *Journal of Photochemistry and Photobiology A: Chemistry*, *433*, 114133.
[66]. Ghosh, S. K., Samanta, S., Hirani, H., & da Silva, C. R. V. (Eds.). (2022). *Effective Waste Management and Circular Economy: Legislative Framework and Strategies*. CRC Press.
[67]. Patra, S., Mallisetty, P. K., Murmu, N. C., Hirani, H., & Samanta, P. (2022). Study on fracture evaluation in hydrogen environment in 316L stainless steel used in high pressure hydrogen tank. *Materials Today: Proceedings*.
[68]. Nag, S., Mondal, U., Hirani, H., Chakraborty, D., Bhaumik, A., & Banerjee, P. (2022). Strategic optimization of phase-selective thermochemically amended terra-firma originating from excavation-squander for geogenic fluoride adsorption: a combined experimental and in silico approach. *Environmental Science and Pollution Research*, 1-18.
[69]. Sadhu, K. K., Bapanapalle, C. O., Hirani, H., Mandal, N., & Sahoo, R. R. (2022). Simultaneous effect of flake powder methodology and SiC addition on the density and hardness of Al matrix. *Materials Today: Proceedings*, *66*, 3897-3901.
[70]. Banerjee, P., Hasda, R., Murmu, M., & Hirani, H. (2022). MgO as corrosion inhibitor. In *Inorganic Anticorrosive Materials* (pp. 183-210). Elsevier.
[71]. Kumar, P., Hirani, H., & Chatterjee, A. (2021). *U.S. Patent No. 10,962,333*. Washington, DC: U.S. Patent and Trademark Office.
[72]. Dey, D., Mondal, A., Nag, S., Mondal, U., Hirani, H., & Banerjee, P. (2021). The designed synthesis of a hydrophobic covalent polymer composite to expel toxic dyes and oil from wastewater: theoretical corroboration. *New Journal of Chemistry*, *45*(11), 5165-5175.
[73]. Chatterjee, D., Dutta, S., Mondal, B., & Hirani, H. (2020). On the Effectiveness of a "Tractor Mounted Road Sanitizing Unit" Designed to Combat COVID-19 Spread. *Journal of The Institution of Engineers (India): Series C*, *101*(6), 1093-1098.
[74]. Lijesh, K. P., & Hirani, H. (2015, November). Effect of dimensional tolerances on the performance of hybrid bearing. In *Proceedings of Malaysian International Tribology Conference* (Vol. 2015, pp. 40-41).
[75]. Sarkar, C., & Hirani, H. (2015). Particle Dynamics of Polydisperse Magnetorheological Fluids. *Smart Science*, *3*(4), 176-187.
[76]. SUKHWANI, V., & HIRANI, H. (2007). Synthesis and characterization of low cost magnetorheological (MR) fluids-art. no. 65262R. SPIE-INT SOC OPTICAL ENGINEERING.
[77]. SUKHWANI, V., & HIRANI, H. Synthesis and characterization of magnetorheological (mr) lubricants.
[78]. Meena, V., & Hirani, H. (2006) Switching amplifier for frictionless BEARING., International conference on Industrial Tribology.
[79]. Samanta, P., & Hirani, H. (2007). A simplified optilviization approach for permanent magnetic journal bearing. Indian Journal of Tribology, Vol 2 No 2.
[80]. Kumar, A., Antil, S. K., Rani, V., Antil, P., Jangra, D., Kumar, R., & Pruncu, C. I. (2020). Characterization on Physical, Mechanical, and Morphological Properties of Indian Wheat Crop. *Sustainability*, *12*(5), 2067.
[81]. Jangra, D., & Muzakkir, S. M. (2022). Failure Modes and Effect Analysis of Gear Pair. *Specialusis Ugdymas*, *2*(43), 901-910.
[82]. Jangra, D., & Muzakkir, S. M. (2022). A Review on Dynamic Response Modelling of Faulted Gearbox. *Specialusis Ugdymas*, *1*(43), 7280-7294.
[83]. Jangra, D. (2022). A Review on Selection of Gear Drive Lubricating Oil. *Int. J. of Multidisciplinary and Current research*, *10*.
[84]. Jangra, D. (2022). Condition Monitoring as Tool of Engineering Management. *Int. J. of Multidisciplinary and Current research*, *10*.
[85]. Jangra, D. (2022). A Review on Different Faults in Gearbox and Vibration Based Diagnosis. *Int. J. of Current Engineering and Technology*
[86]. Jangra, D. (2022). A Review on Tribological Parameters for Fault Diagnosis in Spur Gears. *Int. J. of Current Engineering and Technology*
[87]. Mohammed, O. D., 2015, *Dynamic Modelling and Vibration Analysis for Gear Tooth Crack Detection*.
[88]. Mohammed, O. D., Rantatalo, M., and Kumar, U., 2012, "Analytical Crack Propagation Scenario for Gear Teeth and Time-Varying Gear Mesh Stiffness," pp. 1332–1337.
[89]. Coy, J. J., Townsend, D. P., and Zaretsky, E. V., 2010, "Dynamic Capacity and Surface Fatigue Life for Spur and Helical Gears," J. Lubr. Technol., **98**(2), p. 267.
[90]. Glodez, S., Ren, Z., and Flasï, J., 2000, "Surface Fatigue of Gear Teeth Flanks," Stress Int. J. Biol. Stress, **73**(1999), pp. 475–483.
[91]. Zhu, D., Ren, N., and Wang, Q. J., 2009, "Pitting Life Prediction Based on a 3D Line Contact Mixed EHL Analysis and Subsurface von Mises Stress Calculation," J. Tribol., **131**(4), p. 041501.
[92]. Amarnath, M., Sujatha, C., and Swarnamani, S., 2009, "Experimental Studies on the Effects of Reduction in Gear Tooth Stiffness and Lubricant Film Thickness in a Spur Geared System," Tribol. Int., **42**(2), pp. 340–352.
[93]. Bartz, W. J., and Krijger, V., 1973, "Pitting Fatigue of Gears - Some Ideas on a p p e a r a n c e , m e c h a n i s m and Lubricant Influence," (October), pp. 191–195.
[94]. Townsend, D. P., Zaretsky, E. V., and Scibbe, H. W., 1989, "Lubricant and Additive Effects on Spur Gear Fatigue Life," J. Synth. Lubr., **6**(2), pp. 83–106.
[95]. Krantz, T. L., Alanou, M. P., Evans, H. P., and Snidle, R. W., 2002, "Surface Fatigue Lives of Case-Carburized Gears With an Improved Surface Finish," J. Tribol., **123**(4), p. 709.
[96]. Li, S., 2015, "An Investigation on the Influence of Misalignment on Micro-Pitting of a Spur Gear Pair," Tribol. Lett., **60**(3), pp. 1–12.
[97]. Saxena, A., Chouksey, M., and Parey, A., 2017, "Effect of Mesh Stiffness of Healthy and Cracked Gear Tooth on Modal and Frequency Response Characteristics of Geared Rotor System," Mech. Mach. Theory, **107**(October 2016), pp. 261–273.
[98]. Blake, J. W., and Cheng, H. S., 2008, "A Surface Pitting Life Model for Spur Gears: Part I—Failure Probability Prediction," J. Tribol., **113**(4), p. 719.

[99]. Blake, J. W., and Cheng, H. S., 2008, "A Surface Pitting Life Model for Spur Gears: Part II—Failure Probability Prediction," J. Tribol., **113**(4), p. 719.

[100]. Ramamurti, V., Vijayendra, N. H., and Sujatha, C., 1998, "Static and Dynamic Analysis of Spur and Bevel Gears Using Fem," Mech. Mach. Theory, **33**(8), pp. 1177–1193.

[101]. Kundu, P., Darpe, A. K., and Kulkarni, M. S., 2019, "A Correlation Coefficient Based Vibration Indicator for Detecting Natural Pitting Progression in Spur Gears," Mech. Syst. Signal Process., **129**, pp. 741–763.

[102]. Ognjanovic, M., 2004, "Progressive Gear Teeth Wear and Failure Probability Modeling," Tribol. Ind., **26**(3–4), pp. 44–49.

[103]. Li, S., and Kahraman, A., 2011, "A Fatigue Model for Contacts under Mixed Elastohydrodynamic Lubrication Condition," Int. J. Fatigue, **33**(3), pp. 427–436.

[104]. Goyal, D., Vanraj, Pabla, B. S., and Dhami, S. S., 2017, "Condition Monitoring Parameters for Fault Diagnosis of Fixed Axis Gearbox: A Review," Arch. Comput. Methods Eng., **24**(3), pp. 543–556.

[105]. Amarnath, M., and Lee, S. K., 2015, "Assessment of Surface Contact Fatigue Failure in a Spur Geared System Based on the Tribological and Vibration Parameter Analysis," Measurement, **76**, pp. 32–44.

[106]. Sharma, V., and Parey, A., 2016, "Gear Crack Detection Using Modified TSA and Proposed Fault Indicators for Fluctuating Speed Conditions," Meas. J. Int. Meas. Confed., **90**, pp. 560–575.

[107]. Nanadic, N., Ardis, P., Hood, A., Thurston, M., Ghoshal, A., and Lewicki, D., 2003, "Comparative Study of Vibration Condition Indicators for Detecting Cracks in Spur Gears."

[108]. Dempsey, P. J., 2000, "A Comparison of Vibration and Oil Debris Gear Damage Detection Methods Applied to Pitting Damage," Nasa/Tm-2000-210371, (September), p. 18.

[109]. Cerrada, M., Zurita, G., Cabrera, D., Sánchez, R. V., Artés, M., and Li, C., 2016, "Fault Diagnosis in Spur Gears Based on Genetic Algorithm and Random Forest," Mech. Syst. Signal Process., **70**–**71**, pp. 87–103.

[110]. Igba, J., Alemzadeh, K., Durugbo, C., and Eiriksson, E. T., 2016, "Analysing RMS and Peak Values of Vibration Signals for Condition Monitoring of Wind Turbine Gearboxes," Renew. Energy, **91**, pp. 90–106.

[111]. Verma, A., Zhang, Z., and Kusiak, A., 2013, "Modeling and Prediction of Gearbox Faults With Data-Mining Algorithms," J. Sol. Energy Eng., **135**(3), p. 031007.

[112]. Parey, A., El Badaoui, M., Guillet, F., and Tandon, N., 2006, "Dynamic Modelling of Spur Gear Pair and Application of Empirical Mode Decomposition-Based Statistical Analysis for Early Detection of Localized Tooth Defect," J. Sound Vib., **294**(3), pp. 547–561.

[113]. Saravanan, N., Cholairajan, S., and Ramachandran, K. I., 2009, "Vibration-Based Fault Diagnosis of Spur Bevel Gear Box Using Fuzzy Technique," Expert Syst. Appl., **36**(2 PART 2), pp. 3119–3135.

[114]. Dempsey, and J., P., 2003, "Integrating Oil Debris and Vibration Measurements for Intelligent Machine Health Monitoring. Degree Awarded by Toledo Univ., May 2002," (March).

[115]. Wang, Y., Xiang, J., Markert, R., and Liang, M., 2016, "Spectral Kurtosis for Fault Detection, Diagnosis and Prognostics of Rotating Machines: A Review with Applications," Mech. Syst. Signal Process., **66**–**67**, pp. 679–698.

[116]. Choy, F., Xu, A., and Polyshchuk, V., 2018, "Development of a Model Based Technique for Gear Diagnostics Using the Winger-Ville Method."

[117]. Dempsey, P. J., Mosher, M., and Huff, E. M., 2003, "Threshold Assessment of Gear Diagnostic Tools on Flight and Test Rig Data," NASA/TM, (August).

[118]. Hu, C., Smith, W. A., Randall, R. B., and Peng, Z., 2016, "Development of a Gear Vibration Indicator and Its Application in Gear Wear Monitoring," Mech. Syst. Signal Process., **76**–**77**, pp. 319–336.

[119]. Bartelmus, W., and Zimroz, R., 2009, "A New Feature for Monitoring the Condition of Gearboxes in Non-Stationary Operating Conditions," Mech. Syst. Signal Process., **23**(5), pp. 1528–1534.

[120]. Dalpiaz, G., Rivola, A., and Rubini, R., 2000, "Effectiveness and Sensitivity of Vibration Processing Techniques for Local Fault Detection in Gears," Mech. Syst. Signal Process., **14**(3), pp. 387–412.

[121]. Widodo, A., Satrijo, D., Prahasto, T., and Haryanto, I., 2017, "Fault Detection of Gearbox Using Time-Frequency Method," AIP Conf. Proc., **1831**.

[122]. Halim, E. B., Shoukat Choudhury, M. A. A., Shah, S. L., and Zuo, M. J., 2008, "Time Domain Averaging across All Scales: A Novel Method for Detection of Gearbox Faults," Mech. Syst. Signal Process., **22**(2), pp. 261–278.

[123]. Ziaran, S., and Darula, R., 2013, "Determination of the State of Wear of High Contact Ratio Gear Sets by Means of Spectrum and Cepstrum Analysis," J. Vib. Acoust., **135**(2), p. 021008.

[124]. Zhang, R., Gu, X., Gu, F., Wang, T., and Ball, A., 2017, "Gear Wear Process Monitoring Using a Sideband Estimator Based on Modulation Signal Bispectrum," Appl. Sci., **7**(3), p. 274.

[125]. Urbanek, J., Barszcz, T., Strączkiewicz, M., and Jablonski, A., 2017, "Normalization of Vibration Signals Generated under Highly Varying Speed and Load with Application to Signal Separation," Mech. Syst. Signal Process., **82**, pp. 13–31.

[126]. Teng, W., Ding, X., Zhang, X., Liu, Y., and Ma, Z., 2016, "Multi-Fault Detection and Failure Analysis of Wind Turbine Gearbox Using Complex Wavelet Transform," Renew. Energy, **93**, pp. 591–598.

[127]. Abboud, D., Baudin, S., Antoni, J., Rémond, D., Eltabach, M., and Sauvage, O., 2016, "The Spectral Analysis of Cyclo-Non-Stationary Signals," Mech. Syst. Signal Process., **75**, pp. 280–300.

[128]. Zhu, L., Ding, H., and Zhu, X. Y., 2007, "Synchronous Averaging of Time-Frequency Distribution With Application to Machine Condition Monitoring," J. Vib. Acoust., **129**(4), p. 441.

[129]. Mosher, M., Pryor, A. H., and Lewicki, D. G., 2010, "Detailed Vibration Analysis of Pinion Gear with Time Frequency Methods," Electromagn. Interconnections, (June 2003), pp. 189–217.

[130]. Staszewski, W. J., and Tomlinson, G. R., 1997, "Local Tooth Fault Detection in Gearboxes Using a Moving Window Procedure," Mech. Syst. Signal Process., **11**(3), pp. 331–350.

[131]. Choy, F. K., Mugler, D. H., and Zhou, J., 2003, "Damage Identification of a Gear Transmission Using Vibration Signatures," J. Mech. Des., **125**(2), p. 394.

[132]. W J Staszewski, K Worden, G. R. T., 1997, "Time–Frequency Analysis in Gearbox Fault Detection Using the Wigner–Ville Distribution and Pattern Recognition," Mech. Syst. Signal Process., **11**(5), pp. 673–692.

[133]. Loutridis, S. J., 2006, “Instantaneous Energy Density as a Feature for Gear Fault Detection,” Mech. Syst. Signal Process., **20**(5), pp. 1239–1253.

[134]. Wang, W., and Kanneg, D., 2009, “An Integrated Classifier for Gear System Monitoring,” Mech. Syst. Signal Process., **23**(4), pp. 1298–1312.

[135]. Li, Z., Jiang, Y., Hu, C., and Peng, Z., 2016, “Recent Progress on Decoupling Diagnosis of Hybrid Failures in Gear Transmission Systems Using Vibration Sensor Signal: A Review,” Meas. J. Int. Meas. Confed., **90**, pp. 4–19.

[136]. Peng, Z. K., and Chu, F. L., 2004, “Application of the Wavelet Transform in Machine Condition Monitoring and Fault Diagnostics: A Review with Bibliography,” Mech. Syst. Signal Process., **18**(2), pp. 199–221.

[137]. Rafiee, J., and Tse, P. W., 2009, “Use of Autocorrelation of Wavelet Coefficients for Fault Diagnosis,” Mech. Syst. Signal Process., **23**(5), pp. 1554–1572.

[138]. Yoshida, A., Ohue, Y., and Ishikawa, H., 2000, “Diagnosis of Tooth Surface Failure by Wavelet Transform of Dynamic Characteristics,” Tribol. Int., **33**(3–4), pp. 273–279.

[139]. Fan, X., and Zuo, M. J., 2006, “Gearbox Fault Detection Using Hilbert and Wavelet Packet Transform,” Mech. Syst. Signal Process., **20**(4), pp. 966–982.

[140]. Lin, J., and Zuo, M. J., 2004, “Extraction of Periodic Components for Gearbox Diagnosis Combining Wavelet Filtering and Cyclostationary Analysis,” J. Vib. Acoust., **126**(3), p. 449.

[141]. Li, H., Zhang, Y., and Zheng, H., 2011, “Application of Hermitian Wavelet to Crack Fault Detection in Gearbox,” Mech. Syst. Signal Process., **25**(4), pp. 1353–1363.

[142]. Mark, W. D., 2015, “Time-Synchronous-Averaging of Gear-Meshing-Vibration Transducer Responses for Elimination of Harmonic Contributions from the Mating Gear and the Gear Pair,” Mech. Syst. Signal Process., **62**, pp. 21–29.

[143]. Raad, A., Antoni, J., and Sidahmed, M., 2008, “Indicators of Cyclostationarity: Theory and Application to Gear Fault Monitoring,” Mech. Syst. Signal Process., **22**(3), pp. 574–587.

[144]. Coats, M. D., and Randall, R. B., 2014, “Single and Multi-Stage Phase Demodulation Based Order-Tracking,” Mech. Syst. Signal Process., **44**(1–2), pp. 86–117.

[145]. Pan, M. C., and Lin, Y. F., 2006, “Further Exploration of Vold-Kalman-Filtering Order Tracking with Shaft-Speed Information-II: Engineering Applications,” Mech. Syst. Signal Process., **20**(6), pp. 1410–1428.

[146]. Cheng, W., Zhang, Z., Lee, S., and He, Z., 2012, “Source Contribution Evaluation of Mechanical Vibration Signals via Enhanced Independent Component Analysis,” J. Manuf. Sci. Eng., **134**(2), p. 021014.

[147]. Tumer, I. Y., and Huff, E. M., 2003, “Analysis of Triaxial Vibration Data for Health Monitoring of Helicopter Gearboxes,” J. Vib. Acoust., **125**(1), p. 120.

[148]. Li, B., Zhang, X., and Wu, J., 2017, “New Procedure for Gear Fault Detection and Diagnosis Using Instantaneous Angular Speed,” Mech. Syst. Signal Process., **85**, pp. 415–428.

[149]. Ricci, R., and Pennacchi, P., 2011, “Diagnostics of Gear Faults Based on EMD and Automatic Selection of Intrinsic Mode Functions,” Mech. Syst. Signal Process., **25**(3), pp. 821–838.

[150]. Wu, T. Y., Chen, J. C., and Wang, C. C., 2012, “Characterization of Gear Faults in Variable Rotating Speed Using Hilbert-Huang Transform and Instantaneous Dimensionless Frequency Normalization,” Mech. Syst. Signal Process., **30**, pp. 103–122.

[151]. Mark, W. D., Lee, H., Patrick, R., and Coker, J. D., 2010, “A Simple Frequency-Domain Algorithm for Early Detection of Damaged Gear Teeth,” Mech. Syst. Signal Process., **24**(8), pp. 2807–2823.

[152]. Villa, L. F., Reñones, A., Perán, J. R., and De Miguel, L. J., 2012, “Statistical Fault Diagnosis Based on Vibration Analysis for Gear Test-Bench under Non-Stationary Conditions of Speed and Load,” Mech. Syst. Signal Process., **29**, pp. 436–446.

[153]. Abbes, M. S., Trigui, M., Chaari, F., Fakhfakh, T., and Haddar, M., 2010, “Dynamic Behaviour Modelling of a Flexible Gear System by the Elastic Foundation Theory in Presence of Defects,” Eur. J. Mech. A/Solids, **29**(5), pp. 887–896.

[154]. Mark, W. D., and Hines, J. A., 2014, “Frequency-Domain Assessment of Gear-Tooth Bending-Fatigue Damage-Progression Using the Average-Log-Ratio, ALR, Algorithm,” Mech. Syst. Signal Process., **45**(2), pp. 479–487.

[155]. Li, Y., Ding, K., He, G., and Lin, H., 2016, “Vibration Mechanisms of Spur Gear Pair in Healthy and Fault States,” Mech. Syst. Signal Process., **81**, pp. 183–201.

[156]. Yesilyurt, I., Gu, F., and Ball, A. D., 2003, “Gear Tooth Stiffness Reduction Measurement Using Modal Analysis and Its Use in Wear Fault Severity Assessment of Spur Gears,” NDT E Int., **36**(5), pp. 357–372.

[157]. Amarnath, M., and Sujatha, C., 2015, “Surface Contact Fatigue Failure Assessment in Spur Gears Using Lubricant Film Thickness and Vibration Signal Analysis,” Tribol. Trans., **58**(2), pp. 327–336.

[158]. Ding, H., and Kahraman, A., 2007, “Interactions between Nonlinear Spur Gear Dynamics and Surface Wear,” J. Sound Vib., **307**(3–5), pp. 662–679.

[159]. Yu, W., Mechefske, C. K., and Timusk, M., 2017, “The Dynamic Coupling Behaviour of a Cylindrical Geared Rotor System Subjected to Gear Eccentricities,” Mech. Mach. Theory, **107**(April 2016), pp. 105–122.

[160]. J N, Reddy, “Mechanics of laminated composite plates and shells” 2nd ed., CRC press, pp. 83.

[161]. J N, Reddy, “Mechanics of laminated composite pltes and shelles” 2nd ed., CRC press, pp. 142-144.

[162]. J N,Reddy, “Mechanics of laminated composite pltes and shelles” 2nd ed., CRC press, pp. 112-115.

[163]. J N,Reddy, “Mechanics of laminated composite pltes and shelles” 2nd ed., CRC press, pp. 115-129.

[164]. J N,Reddy, “Mechanics of laminated composite pltes and shelles” 2nd ed., CRC press, pp. 132-140.

[165]. J N,Reddy, “Mechanics of laminated composite pltes and shelles” 2nd ed., CRC press, pp. 404.

[166]. F.Auricchio and E.Sacco,”Redefined first order shear deformation theory models for composite laminates” in applied mechanics , vol.70,2004,pp.380-390.

[167]. B. S. Reddy,J.S Kumar,C.E. Reddy and K.V.K. Reddy,” Static analysis of functionaly graded plate using higher order shear deformation theory” applied science and engineering,2013,23-41.